ISSN 1063-7834, Physics of the Solid State, 2013, Vol. 55, No. 7, pp. 1401–1406. © Pleiades Publishing, Ltd., 2013.
Original Russian Text © D.A. Balaev, O.A. Bulavchenko, A.A. Dubrovskii, S.V. Tsybulya, S.V. Cherepanova, E.Yu. Gerasimov, K.A. Shaikhutdinov, 2013, published in Fizika Tverdogo Tela, 2013, Vol. 55, No. 7, pp. 1304–1309.

MAGNETISM

# Features of the Structure, Microstructure, and Magnetic Properties of Manganese–Aluminum Spinels Obtained in Various Thermal Treatment Conditions

**D. A. Balaev[a], O. A. Bulavchenko[b, c], A. A. Dubrovskii[a], S. V. Tsybulya[b, c], S. V. Cherepanova[b, c], E. Yu. Gerasimov[b], and K. A. Shaikhutdinov[a]**

[a] *Kirensky Institute of Physics, Siberian Branch of the Russian Academy of Sciences, Akademgorodok 50–38, Krasnoyarsk, 660036 Russia*
*e-mail: smp@iph.krasn.ru*

[b] *Boreskov Institute of Catalysis, Siberian Branch of the Russian Academy of Sciences, pr. Akademika Lavrentieva 5, Novosibirsk, 630090 Russia*

[c] *Novosibirsk State University, ul. Pirogova 2, Novosibirsk, 630090 Russia*

Received January 9, 2013

**Abstract**—The structural, microstructural, and magnetic properties of aluminum–manganese oxide in the ratio Mn : Al = 1 : 1 in the well-crystallized and nanoheterogeneous states have been investigated. This oxide is obtained under various thermal treatment conditions and at different partial pressures of oxygen. The composition and cation distribution of the manganese and aluminum ions in spinel sites are determined. It is shown that the studied compound is a ferrimagnet with the Curie point $T_C \approx 26$ K.

**DOI:** 10.1134/S1063783413070056

## 1. INTRODUCTION

Physical properties of manganese oxides are currently of great interest because of the prospects of potential use of these materials for high-density magnetic recording, in electrochemical facilities, in chemical industry, etc. Particularly, the Al–Mn oxides are used as the catalysts for the complete oxidation of CO and hydrocarbons [1–4].

The specific features of the behavior of manganese-containing mixed oxides are associated with their ability to loss or attach oxygen in particular temperature ranges and media with the corresponding variation in the degree of oxidation of manganese ions. As a consequence, manganese-containing solid solutions with the spinel structure decompose with the formation of nanostructured states particularly due to the separation of the β-$Mn_3O_4$ particles [5, 6]. The assumed cause of such decomposition is the tendency of the $Mn^{3+}$ cations to segregate due to the cooperative Jahn–Teller effect.

We previously showed for the $Mn_{1.5}Al_{1.5}O_4$ system that the ordered spinel with the content of manganese ions of the order of 50% decomposes to the nanostructured state, which is accompanied by the attachment of oxygen and the variation in the degree of oxidation of manganese [5, 6]. Particularly, it was shown using the X-ray structural data [5] that the initial $Mn_{1.5}Al_{1.5}O_4$ system, being affected by a high temperature in air, transforms into two spinel structures β-$Mn_3O_4$ and $Mn_{0.4}Al_{2.4}O_4$. The investigation of magnetic properties of these systems can confirm and complement the previous information on the features of the structural transformations and the valence of manganese in mentioned oxides. Manganese cations in the $Mn_{1.5}Al_{1.5}O_4$ system are arranged both in the octahedral and tetrahedral spinel sites. Therefore, the investigation of the magnetic properties of this composition is of the separate interest since the attention was paid in publications to the substitution of manganese in one site (either in the octahedron or in the tetrahedron).

In this article, we present the results of studying the structure, the microstructure, and the magnetic properties of the systems with the atomic ratio Mn : Al = 1 : 1 with the regular structure of spinel $Mn_{1.5}Al_{1.5}O_4$ and in the nanoheterogeneous state obtained after the thermal treatment.

## 2. EXPERIMENT

### *2.1. Preparation Procedure*

The sample with the atomic ratio Mn : Al = 1 : 1 was prepared by the joint deposition of manganese and aluminum hydroxides by ammonia from solutions of $Al(NO_3)_3$ and $Mn(NO_3)_2$ under stirring with a rate of 550 $min^{-1}$ until pH = 10 was attained. Then the precipitate was aged at 70–80°C for 1 h. Then the residue was filtered, washed with distilled water to pH = 6, and dried at 120°C. The dried residue was triturated in a

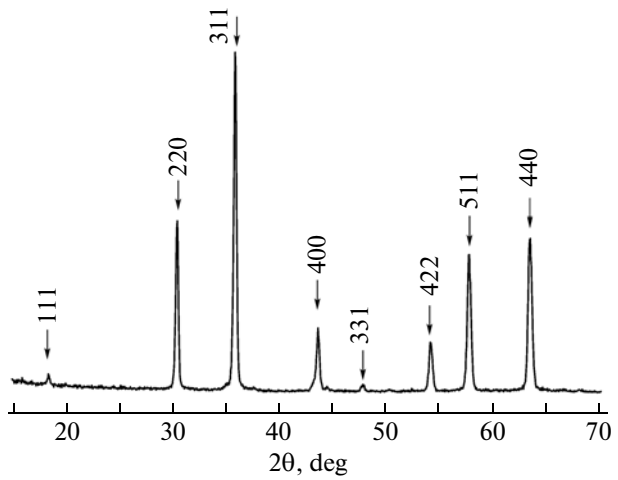


**Fig. 1.** Diffraction pattern of the initial $Mn_{1.5}Al_{1.5}O_4$ sample.

mortar and calcined at 300°C for 4 h. After this, the powder was calcined in air at 700°C for 4 h and then in argon at 1050°C for 4 h. Then the samples were calcined in air at 700°C for 4 h. We further call such sample as calcined, while the initial sample is denoted as $Mn_{1.5}Al_{1.5}O_4$.

### *2.2. X-Ray Diffractometry*

The diffraction studies were performed using a D8 diffractometer (Bruker, Germany) using an Anton Paar high-temperature X-ray chamber (Austria). The diffractometer is equipped by the Göbel mirror (Bruker, Germany), which forms a parallel X-ray beam. We used Cu$K_\alpha$ radiation with wavelength $\lambda$ = 1.5418 Å.

The cell parameters and the structure were refined using the POLYCRYSTAL program [7]. The contents of manganese and aluminum ions in the solid solution with the spinel structure were determined by the dependence of the unit cell volume on the Mn : Al ratio constructed with the use of the reference data ($\gamma$-$Al_2O_3$, $\gamma$-$Mn_3O_4$, $Mn_2AlO_4$, and $MnAl_2O_4$ [8]) in the linear approximation. The average size of the coherent scattering region (CSR) was determined by the Scherrer formula.

### *2.3. Electron Microscopy*

The high-resolution transmission electron microscopy (HRTEM) was used to obtain the detail information on the sample morphology and the structure. For these studies, we used a JEM2010 transmission electron microscope with the resolution by the lines of 1.4 Å and the accelerating voltage of 200 kV. The phases were identified and their actual structure was investigated using the electron diffraction in the separated region. The Fourier numerical analysis was used to analyze the HRTEM microphotographs.

### *2.4. Measurement of the Magnetic Properties*

The temperature dependences of the magnetic moment $M(T)$ and the dependences of the magnetic moment on the external field (isothermal $M(H)$) were measured using the vibrational magnetometer [9]. Dependences $M(T)$ were measured in cooling modes to $T$ = 4.2 K in the zero-field-cooled (ZFC) and field-cooled (FC) modes. The samples (the powder) 10–20 mg in weight were fixed in a measuring capsule with paraffin. The data were corrected to the diamagnetic capsule signal.

## RESULTS AND DISCUSSION

### *3.1. Structural Characteristics of the Initial Spinel $Mn_{1.5}Al_{1.5}O_4$ and the Calcined Sample*

Figure 1a shows the X-ray diffraction pattern of the initial sample, and narrow peaks of the cubic phase belonging to the spinel structural type (space group *Fd*3*m*) are observed. The unit cell parameter was 8.285(1) Å, and the CSR average size was more than 150 nm. The contents of the manganese and aluminum ions in the spinel-type solid solution were determined by the dependence of the reduced unit cell volume on the content of the aluminum ions in $Mn_{3-x}Al_xO_4$ (Fig. 2a) constructed with the use of the reference data [8]. It follows from Fig. 2 that the reduced volume ($a$ = 8.285(1) Å, $V^*$ = 284.4 Å$^3$) corresponds to the composition $Mn_{1.5}Al_{1.5}O_4$. The crystal structure was refined with varying the distribution of the manganese and aluminum cations over the octahedral (*B*) and tetrahedral (*A*) sites as well as of thermal factors $B_j$ and oxygen atomic coordinates ($x$, $x$, $x$). The results of calculation are presented in Table 1; invalidity factor $R_I$ of the model was 1.5%. It is seen that the

**Table 1.** Crystal structure of $Mn_{1.5}Al_{1.5}O_4$

| Site | Composition | Coordinate | | | Population | Thermal parameter | $R_T$ factor, % |
|---|---|---|---|---|---|---|---|
| | | $x$ | $y$ | $z$ | | | |
| *A* | 0.7Mn + 0.3Al | 0.125 | 0.125 | 0.125 | 1.0(1) | 0.2(1) | |
| *B* | 0.8Mn + 1.2Al | 0.5 | 0.5 | 0.5 | 1.0(1) | 0.5(1) | 1.5 |
| *O* | 4O | 0.263(1) | 0.263(1) | 0.263(1) | 1.0(1) | 1.3(1) | |

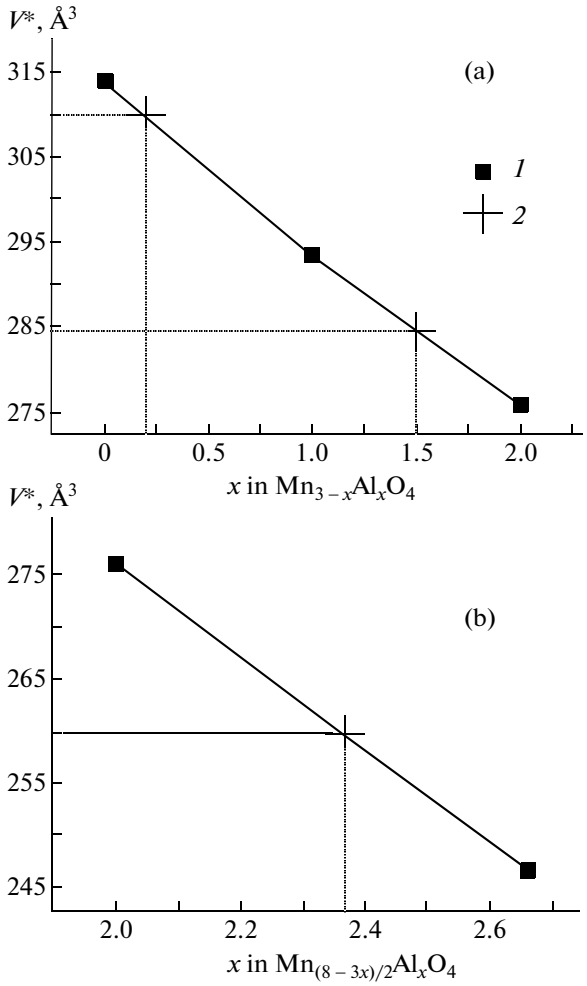


**Fig. 2.** Composition dependences of the reduced unit cell volume (a) in $Mn_{3-x}Al_xO_4$ at $x = 0–2$ and (b) in $Mn_{(8-3x)/2}Al_xO_4$ at $x = 2.00–2.67$. (*1*) Reference data for $Mn_3O_4$, $Mn_2AlO_4$, $MnAl_2O_4$, and $Al_2O_3$; and (*2*) the experimental results.

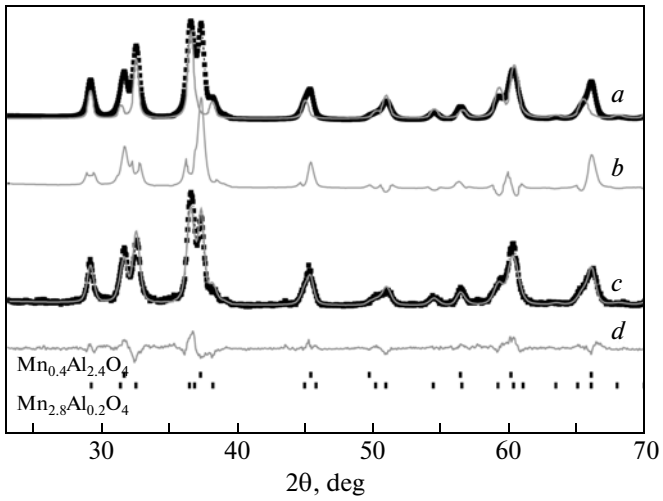


**Fig. 3.** Diffraction pattern refinement using the Rietveld method for the calcined sample. The models of (*a*) tetragonal spinel β-$Mn_3O_4$ and (*c*) the mixture of the tetragonal ($Mn_{2.8}Al_{0.2}O_4$) and cubic ($Mn_{0.4}Al_{2.4}O_4$) spinels. (*b*, *d*) Difference curves between the experiment and these models. The dashes denote the peak locations for the tetragonal ($Mn_{2.8}Al_{0.2}O_4$) and cubic ($Mn_{0.4}Al_{2.4}O_4$) spinels.

manganese and aluminum cations are arranged isomorphically by the sites, which contain 0.7Mn + 0.3Al in the tetrahedral sites and 0.8Mn + 1.2Al in the octahedral sites, i.e., the $Mn_{1.5}Al_{1.5}O_4$ chemical compound can be written as $(Mn_{0.7}Al_{0.3})[Mn_{0.4}Al_{0.6}]_2O_4$, where the octahedral site is bracketed and the tetrahedral one is parenthesized. Figure 3 shows the X-ray diffraction pattern of the calcined sample. The Rietveld refinement shows the presence of two spinel-type phases. It is seen that the model diffraction pattern of the β-$Mn_3O_4$-type structure does not describe the experimental data completely, and the peaks arranged at angles 2θ of 31.5, 37.1, 45.1, 56.1, and 66.2° remain unrefined. These reflections are indexed in the face-centered cubic cell with the parameter of 8.040(3) Å. The addition of the cubic spinel leads to the better description of the experimental diffraction profile. The results of refining the structural parameters are presented in Table 2. The chemical composition of mixed oxides was evaluated from the unit cell volume reduced to one formula unit. The tetragonal ($Mn_{2.8}Al_{0.2}O_4$) and cubic ($Mn_{0.4}Al_{2.4}O_4$) spinels in a weight ratio of approximately 1 : 1 are present in the calcined sample. The average CSR sizes were evaluated to be 20 and 50 nm for $Mn_{2.8}Al_{0.2}O_4$ and $Mn_{0.4}Al_{2.4}O_4$, respectively.

### *3.2. Microstructural Characteristics*

Figures 4 and 5 show the electron microscopy images of the samples under study. The initial sample

**Table 2.** Results of refinement of structural parameters of the studied samples

| Sample | Phase composition | Lattice parameters, Å | Reduced unit cell volume, Å$^3$ | CSR, nm |
|---|---|---|---|---|
| Initial | $Mn_{1.5}Al_{1.5}O_4$ (cubic spinel) | $a = 8.285(1)$ | 284.4 | >150 |
| Calcined | $Mn_{2.8}Al_{0.2}O_4$ (tetragonal spinel of the β-$Mn_3O_4$ type) | $a = b = 5.721(1)$, $c = 9.471(2)$ | 310.0 | 20 |
| | $Mn_{0.4}Al_{2.4}O_4$ (cubic spinel) | $a = 8.040(3)$ | 259.9 | 50 |

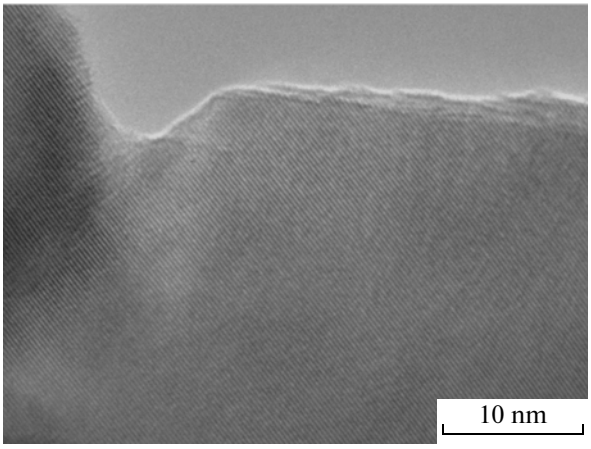


**Fig. 4.** Electron microscopy image of the initial $Mn_{1.5}Al_{1.5}O_4$ sample.

is the well-crystallized spinel with particle sizes >150 nm (Fig. 4).

The particles with the β-$Mn_3O_4$ appear at the calcination temperature of 700°C, as it is seen from the electron-microscopy image; cubic spinel with extended defects is also present (Fig. 5). The X-ray phase analysis data (Table 2) show that two spinel-type phases are present in the calcined sample, namely, tetragonal $Mn_{2.8}Al_{0.2}O_4$ and cubic $Mn_{0.4}Al_{2.4}O_4$.

### *3.3. Magnetic Properties*

Dependences of the magnetic moment in external field $H = 1$ kOe at various magnetic prehistories of the studied samples are presented in Fig. 6. The studied samples displayed the presence of the magnetic transition. Dependences $M(T)$ for the initial $Mn_{1.5}Al_{1.5}O_4$ composition in various modes display the feature, namely, the change of the curvature sign ($d^2M(T)/dT^2 = 0$) at $T \approx 26$ K. Dependences $M(T)$ for the FC and ZFC modes diverge at a lower temperature. Magnetization curve $M(H)$ of this sample at $T =$ 4.2 K, which is shown in Fig. 7, displays the hysteresis; the coercive force is ~1.1 kOe. The shape of hysteresis dependence $M(H)$ as well as the trend of the $M(T)$ curve indicate that the ferrimagnetic ordering type is implemented for this compound.

To obtain the information on the manganese distribution over the cation sites in $Mn_{1.5}Al_{1.5}O_4$, the $M(T)$ dependence for the initial sample in the high-temperature region was analyzed in the context of the Curie–Weiss (CW) classic law $\chi(T) = C/(T - \Theta)$. Here, $C$ is the Curie constant, $C = \mu_B^2 g S(S + 1)/\{3k_B(T - \Theta)\}$, $\mu_B$ is the Bohr magneton, $S$ is the spin value, $g$ factor is 2 for the manganese ions [10], $k_B$ is the Boltzmann constant, and $\Theta$ is the CW paramagnetic temperature. Dependence $\chi^{-1}(T)$ for the initial sample is presented in Fig. 8. It is seen that the CW law is fulfilled at tem-

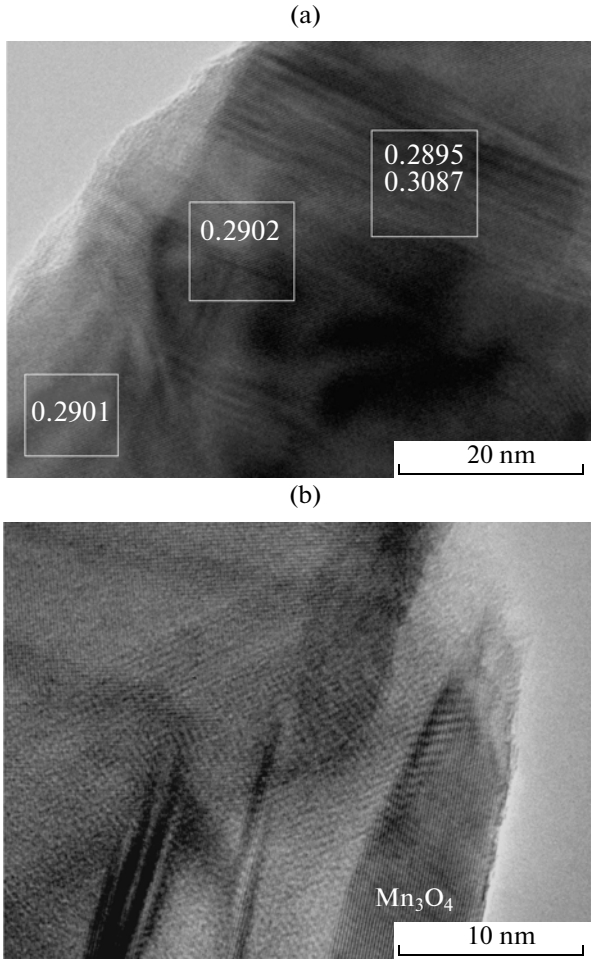


**Fig. 5.** Electron microscopy images of the calcined sample. (a, b) Different sample segments. The numbers correspond to interplanar distances (in nm) in different regions.

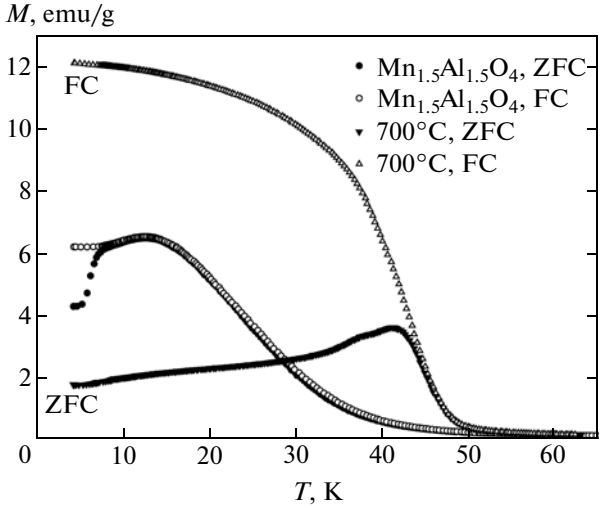


**Fig. 6.** Temperature dependences of the magnetic moment in field $H = 1$ kOe for the initial ($Mn_{1.5}Al_{1.5}O_4$) and calcined samples in the FC and ZFC conditions.

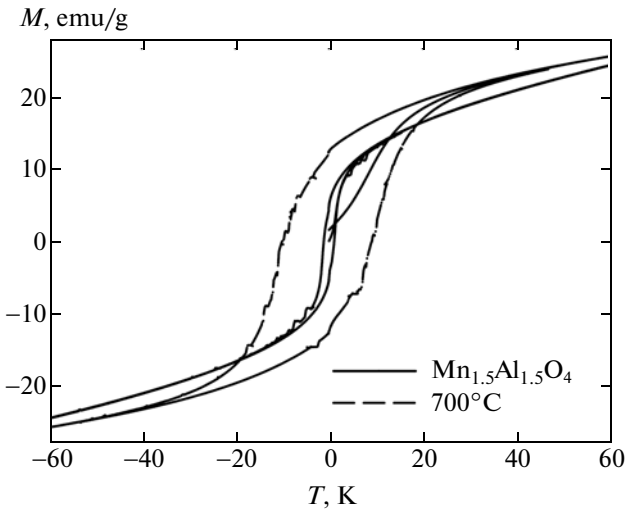


**Fig. 7.** Hysteresis loops $M(H)$ for the initial ($Mn_{1.5}Al_{1.5}O_4$) and calcined samples at $T = 4.2$ K.

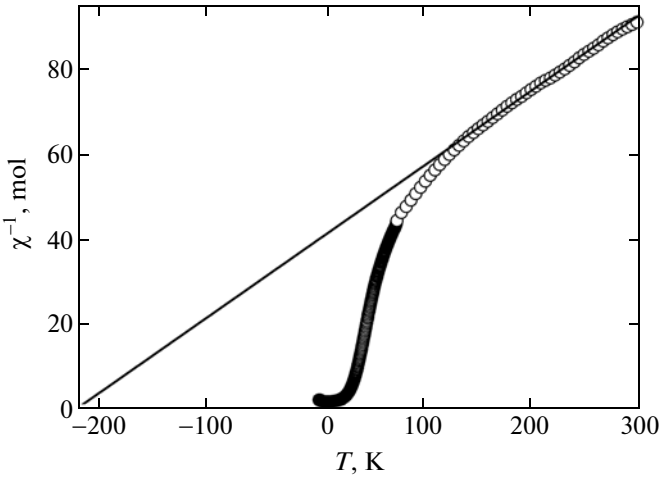


**Fig. 8.** Temperature dependence of the inverse susceptibility for the initial $Mn_{1.5}Al_{1.5}O_4$ sample. $H = 1$ kOe. The line corresponds to the data extrapolation according to the Curie–Weiss law.

peratures above 130 K. Agreement is good at $C = 5.6$ and $\Theta \approx -215$ K (Fig. 8).

Various possibilities are considered, where constant $C$ can be determined by the superposition of various states of the charge and spin of manganese ($Mn^{2+}$, $S = 5/2$; $Mn^{3+}$, $S = 4/2$; $Mn^{4+}$, $S = 3/2$). At two "extreme" variants (the presence of $Mn^{2+}$ and $Mn^{3+}$ only or $Mn^{2+}$ and $Mn^{4+}$), we find $0.78Mn^{2+}$ and $0.72Mn^{3+}$ or $1.12Mn^{2+}$ and $0.38Mn^{4+}$, respectively. However, the electroneutrality condition is not fulfilled, and the excess positive charge is 0.20–0.26. This indicates the presence of cation vacancies in the spinel structure, a small number of which can be unexpressed in the diffraction pattern if they are distributed uniformly over the octahedral and tetrahedral sites. When allowing for 0.06 cation vacancies, 1.47Mn and 1.47Al can be present in the spinel structure. The electroneutrality condition is fulfilled for such a number of vacancies, while the CW constant agrees with the experimental one if we consider than 0.81 of manganese is in the degree of oxidation of 2+, and 0.66 of manganese is in the degree of oxidation of 3+.[1] This result for the charge state of manganese agrees well with the X-ray structural analysis data (Table 1) and allows us to assume the presence of cation vacancies (of about 2%). From the aforesaid, we can propose the following formula:

$(Mn^{2+}_{0.69}Al^{3+}_{0.29}\square_{0.02})[Mn^{2+}_{0.06}Mn^{3+}_{0.33}Al^{3+}_{0.59}\square_{0.02}]_2O_4$ (here, $\square$ is the vacancy).

The $MnAl_2O_4$ compound (cubic spinel), in which the divalent manganese occupies the tetrahedral sites, is the antiferromagnet with the Néel temperature of about 40 K [11]. According to the magnetic and neutron diffraction data [12, 13], the part of $Mn^{2+}$ ions behave paramagnetically up to liquid-helium temperatures. In our case, a considerable number of manganese ions occupy the tetrahedral sites. This apparently promotes the establishment of the ferrimagnetic order in our sample (no paramagnetic contribution is observed at low temperatures).

The magnetic transition temperature for the calcined sample (700°C), which is determined in the point of the change of the curvature sign of the $M(T)$ dependence (Fig. 6), was ~43 K in the FC conditions. This value coincides with the Curie point of the ferrimagnetic transition of the β-$Mn_3O_4$ phase after calcining the initial sample (Fig. 5, Table 2). The temperature dependence of the inverse susceptibility is linear at temperatures higher than ~150 K; these facts are characteristic of polycrystalline $Mn_3O_4$. An anomaly in the vicinity of $T \approx 38$ K, which can correspond to the magnetic transition into the incommensurable spiral structure [10, 14, 15] and manifests itself in dependences $M(T)$, is clearly seen in the $M(T)_{ZFC}$ dependence of the sample calcined at 700°C. It follows from the analysis of the crystallographic data (Table 2) that the regions of tetragonal spinel (of about 20 nm) have the composition $Mn_{2.8}Al_{0.2}O_4$. It seems likely that so light doping with aluminum does not lead to a noticeable shift of the Curie temperature for $Mn_3O_4$. The coercive force of the hysteresis loop of magnetization $M(H)$ of the calcined sample at $T = 4.2$ K is ~9.3 kOe (Fig. 7), which is typical of polycrystalline $Mn_3O_4$. The value of $M$ (4.2 K, 50 kOe) (~25 emu/g) is approximately 60% of the data known from publications for the $Mn_3O_4$ polycrystals [16] and gives the evaluation of the amount of the $Mn_3O_4$ phase in this

[1] An excess positive charge appears with the formal substitution of $2Mn^{3+}$ by $Mn^{2+}$ and $Mn^{4+}$.

sample close to that obtained from the X-ray structural analysis.

The X-ray structural analysis evidences that the aluminum-enriched cubic spinel $Mn_{0.4}Al_{2.4}O_4$ is present in the calcined sample (700°C) in addition to the β-$Mn_3O_4$ tetragonal phase (Table 2). The absence of other clear anomalies (excluding the above-mentioned ones, which are characteristic of $Mn_3O_4$) in dependences $M(T)$ for this sample allows us to assume that the $Mn_{0.4}Al_{2.4}O_4$ compound do not most likely display the magnetic transition, at least to 4.2 K.[2] This fact correlates with the known data on the influence of the diamagnetic substitution (for example, for Zn and Mn) of spinel $Mn_3O_4$ on the Curie temperature [17, 18].

## 4. CONCLUSIONS

Summing these results, we can conclude the following.

(i) The initial aluminum–manganese compound (ratio Mn : Al = 1 : 1) decomposes into two spinel structures after the thermal treatment in air at 700–900°C, namely, $Mn_{2.8}Al_{0.2}O_4$ (tetragonal spinel of the β-$Mn_3O_4$ type) and $Mn_{0.4}Al_{2.4}O_4$ (the cubic spinel) with the crystallites 20 and 50 nm in size. This is confirmed by the structural, microstructural, and magnetic data.

(ii) The composition and the cation distribution in the initial aluminum–manganese spinel (ratio Mn : Al = 1 : 1) are refined with the use of the analysis of the structural data and magnetic measurements. This compound with the chemical formula $Mn^{2+}_{0.69}Al^{3+}_{0.29}(Mn^{2+}_{0.06}Mn^{3+}_{0.33}Al^{3+}_{0.59})_2O_4$ is the ferrimagnet with the Curie temperature of ~26 K.

## ACKNOWLEDGMENTS

We thank T.N. Afonasenko and P.G. Tsyrul'nikov for the synthesis of the samples.

This study was supported by the Russian Foundation for Basic Research (project no. 12-03-90839-mol_rf_nr) and the Ministry of Education and Science of the Russian Federation (agreement no. 8429).

## REFERENCES

1. F. Kapteijn, L. Singoredjo, A. Andreini, and J. A. Moulijn, Appl. Catal., B **3**, 173 (1994).
2. V. A. de la Pena O'Shea, M. C. Alvarez-Galvan, J. L. G. Fierro, and P. L. Arias, Appl. Catal., B **57**, 191 (2005).
3. P. G. Tsyrul'nikov, V. S. Sal'nikov, V. A. Drozdov, S. A. Stuken, A. V. Bubnov, E. I. Grigorov, A. V. Kalinkin, and V. I. Zaikovskii, Kinet. Katal. **32** (2), 439 (1991).
4. J. Carno, M. Ferrandon, E. Bjornbom, and S. Jaras, Appl. Catal., A **155** (2), 265 (1997).
5. O. A. Bulavchenko, S. V. Tsybulya, P. G. Tsyrul'nikov, T. N. Afonasenko, S. V. Cherepanova, and E. Yu. Gerasimov, J. Struct. Chem. **51** (3), 500 (2010).
6. O. A. Bulavchenko, S. V. Tsybulya, E. Yu. Gerasimov, S. V. Cherepanova, T. N. Afonasenko, and P. G. Tsyrulnikov, Z. Kristallogr. Proc. **2011**, 325 (2011).
7. S. V. Tsybulya, S. V. Cherepanova, and L. P. Solov'eva, J. Struct. Chem. **37** (2), 332 (1996).
8. *Joint Committee on Powder Diffraction Standards—International Centre for Diffraction Data, Powder Diffraction Files* (JCPDS–ICDD, Newtown Square, Pennsylvania, United States), PDF Nos. 100425, 130162, 290881, 290880.
9. A. D. Balaev, Yu. V. Boyarshinov, M. M. Karpenko, and B. P. Khrustalev, Prib. Tekh. Eksp., No. 3, 167 (1985).
10. G. Srinivasan and M. S. Seehra, Phys. Rev. B: Condens. Matter **28** (1), 1 (1983).
11. N. Tristan, J. Hemberger, A. Krimmel, H.-A. Krug von Nidda, V. Tsurkan, and A. Loidl, Phys. Rev. B: Condens. Matter **72**, 174404 (2005).
12. G. M. Kalvius, A. Krimmel, O. Hartmann, F. J. Litterst, R. Wappling, V. Tsurkan, and A. Loidl, Physica B (Amsterdam) **404**, 660 (2009).
13. A. Krimmel, V. Tsurkan, D. Sheptyakov, and A. Loidl, Physica B (Amsterdam) **378–380**, 583 (2006).
14. R. Tackett, G. Lawes, B. C. Melot, M. Grossman, E. S. Toberer, and R. Seshadri, Phys. Rev. B: Condens. Matter **76**, 024409 (2007).
15. M. Kim, X. M. Chen, X. Wang, C. S. Nelson, R. Budakian, P. Abbamonte, and S. L. Sooper, Phys. Rev. B: Condens. Matter **84**, 174424 (2011).
16. L. Sicard, J.-M. Le Meins, C. Methivier, F. Herbst, and S. Ammar, J. Magn. Magn. Mater. **322**, 2634 (2010).
17. P. Ghigna, R. De Renzi, M. C. Mozzati, A. Lascialfari, G. Allodi, M. Bimbi, C. Mazzoli, L. Malavasi, and C. B. Azzoni, Phys. Rev. B: Condens. Matter **73**, 184402 (2006).
18. D. P. Shoemaker, E. E. Rodriguez, R. Seshadri, I. S. Abumohor, and T. Proffen, Phys. Rev. B: Condens. Matter **80**, 144422 (2009).

[2] The same phase composition and similar magnetic characteristics are observed when calcining the sample at 900°C.

*Translated by N. Korovin*